Title
Modulation of Survival Motor Neuron Pre-mRNA Splicing by Inhibition of Alternative 3′ Splice Site Pairing*

Journal
Journal of Biological Chemistry, 276(48)

ISSN
0021-9258

Authors
Lim, Sharlene R
Hertel, Klemens J

Publication Date
2001-11-01

DOI
10.1074/jbc.m107632200

THE JOURNAL OF BIOLOGICAL CHEMISTRY
Vol. 276, No. 48, Issue of November 30, pp. 45476–45483, 2001
Printed in U.S.A.

Modulation of Survival Motor Neuron Pre-mRNA Splicing by Inhibition of Alternative 3′ Splice Site Pairing*

Received for publication, August 9, 2001, and in revised form, September 26, 2001
Published, JBC Papers in Press, October 2, 2001, DOI 10.1074/jbc.M107632200

Sharlene R. Lim and Klemens J. Hertel‡

From the Department of Microbiology and Molecular Genetics, College of Medicine, University of California, Irvine, California 92697-4025

Spinal muscular atrophy is caused by the loss of functional survival motor neuron (*SMN1*) alleles. A translationally silent nucleotide transition in the duplicated copy of the gene (*SMN2*) leads to exon 7 skipping and expression of a nonfunctional gene product. It has been suggested that differential *SMN2* splicing is caused by the disruption of an exonic splicing enhancer. Here we show that the single nucleotide difference reduces the intrinsic strength of the 3′ splice site of exon 7 2-fold, whereas the strength of the 5′ splice site of the exon 7 is not affected. Thus, a decrease in splice site strength is magnified in the context of competing exons. These data suggest that lower levels of exon 7 definition not only reduce intron 6 removal but, more importantly, increase the efficiency of the competing exon 7 skipping pathway. Antisense oligonucleotides were tested to modulate exon 7 inclusion, which contains the authentic translation stop codon. Oligonucleotides directed toward the 3′ splice site of exon 8 were shown to alter *SMN2* splicing in favor of exon 7 inclusion. These results suggest that antisense oligonucleotides could be used as a therapeutic strategy to counteract the progression of SMA.

Proximal spinal muscular atrophy (SMA)[1] is a common human genetic disease that is the leading cause of hereditary infant mortality (1–3). It is characterized by the progressive degeneration of the anterior horn stem cells of the spinal cord with consequent paralysis of the trunk and limbs. Three clinical groups of the disease (I-III) have been described based on the decreasing severity of the symptoms (4). SMA has been linked to deletions or mutations of the survival of motor neuron (SMN) gene, which has been mapped as an inverted repeat to chromosome 5 at 5q13 (4). Homozygous absence of the telomeric copy (*SMN1*) correlates with development of SMA (5, 6). By contrast, alterations within the centromeric SMN gene (*SMN2*) do not produce any known phenotype (4). It has been demonstrated that SMN levels produced from the *SMN2* locus modify the severity of the disease in a dose-dependent manner (7, 8). However, *SMN2* alone cannot provide protection from SMA (9–11).

The majority of the SMN transcript consists of 9 exons encoding for a 294-amino acid (38 kDa) gene product. The ubiquitously expressed protein is detected at especially high levels in neuronal cells (7, 8). Until recently, it was unclear why only mutations in the telomeric *SMN1* mutations result in SMA. A genomic sequence comparison of the two genes revealed that *SMN1* and *SMN2* encode for the identical protein (12). However, three alternatively spliced transcripts generated with different efficiencies have been described for each locus (4). *SMN1* primarily produces the full-length form of SMN, whereas differential splicing of the *SMN2* pre-mRNA predominantly produces an isoform lacking exon 7 (SMNΔ7). Comparison of SMN transcripts revealed a direct relationship between SMA and exon 7 skipping. Furthermore, it was demonstrated that SMNΔ7 is unable to efficiently self-associate, a property that correlates with disease severity (13). Thus, SMNΔ7 is not functionally equivalent to full-length SMN, and the failure of *SMN2* to fully compensate for mutations in *SMN1* is because of a differential pre-mRNA-splicing event.

The only critical nucleotide change between *SMN1* and *SMN2* affecting the inclusion of exon 7 has been pinpointed to a single C to T base difference located six nucleotides inside exon 7 (12, 14) (Fig. 1). This transition may disrupt a putative exon-splicing enhancer (ESE) (14), a cis-acting element that generally serves as binding sites for members of the serine-arginine (SR)-rich family of splicing factors (15). An assembled splicing enhancer complex in turn promotes splice site and exon recognition by assisting in the recruitment of the splicing machinery to the adjacent intron through protein-protein interactions (16, 17). Previous work demonstrated that the recognition of weak splice site signals could be aided significantly by the presence of ESEs. By contrast, ESEs have little or no detectable effect on the activation of strong splice sites that conform to the consensus sequence (15–18). Most ESEs studied in mechanistic detail activate 3′ splice sites that contain suboptimal polypyrimidine tracts (py), a stretch of nucleotides immediately upstream of the exon/intron junction. Because py tracts and the 3′ splice site serve as binding sites for the U2 small nuclear ribonucleoprotein auxiliary factor (U2AF) (19–23), a model has emerged suggesting that enhancer complexes assembled on ESEs recruit U2AF to a weak 3′ splice site (24–26). In the case of *SMN2*, it was suggested that the C to T nucleotide difference in exon 7 might disrupt the integrity of a putative ESE to a degree that renders spliceosomal assembly and exon 7 recognition insignificant (12, 14). As a consequence, exon 7 is skipped in *SMN2*, and SMNΔ7 is the product of the alternative processing event. A recent report has tested this hypothesis and demonstrated the presence of an ESE within exon 7 (27). However, the critical C to T transition observed between *SMN1* and *SMN2* was not contained within this re-

* This work was supported by the Families of Spinal Muscular Atrophy. The costs of publication of this article were defrayed in part by the payment of page charges. This article must therefore be hereby marked "*advertisement*" in accordance with 18 U.S.C. Section 1734 solely to indicate this fact.

‡ To whom correspondence should be addressed. Tel.: 949-824-2127; Fax: 949-824-8598; E-mail: khertel@uci.edu.

[1] The abbreviations used are: SMA, spinal muscular atrophy; SMN, survival of motor neuron; *SMN1*, telomeric copy of SMN; *SMN2*, centromeric copy of SMN; ESE, exonic splicing enhancer; py, polypyrimidine tract; 3′ss, 3′ splice site; 5′ss, 5′ splice site; HPRT, hypoxanthine phosphoribosyltransferase; PCR, polymerase chain reaction; bp, branch point; jnct, junction.

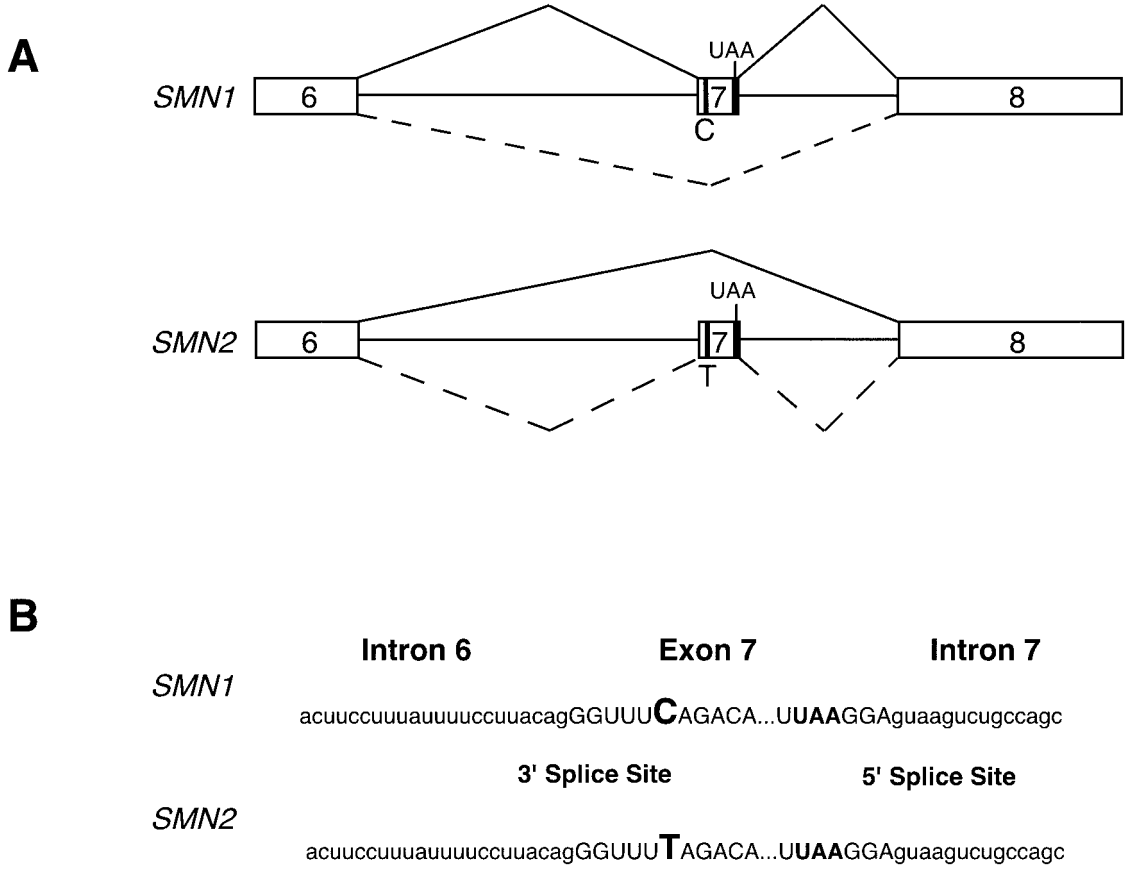

FIG. 1. **Comparison of the *SMN1* and *SMN2* genes.** *A*, schematic of *SMN* mini-gene constructs containing the C to T transition within exon 7 and their preferred splicing pathways. *Solid lines* represent major pathways, and *dotted lines* represent minor pathways. The *thick bars* within exon 7 highlight the position of the C to T transition and the UAA translation stop codon. *B*, *SMN* RNA sequences of the region including exon 7. Exon 7 sequences are in *uppercase*. Intron sequences are in *lowercase*. The C to T transition is highlighted by the large font, and the UAA stop codon at the 3′ end of exon 7 is represented in both.

gion. In fact, within the nucleotide sequences around the C to T transition, no detectable ESE activities were observed. Thus, it is still unclear why the C to T transition leads to exon 7 skipping in *SMN2*.

Because *SMN2* cannot compensate for mutations within *SMN1*, *SMN1* is the SMA-determining gene. More importantly, however, because all individuals with SMA have retained their *SMN2* allele, therapy directed toward increasing *SMN2* exon 7 inclusion could provide a promising tool to lower the clinical severity of SMA. Recent studies have demonstrated that overexpression of hTra2, a splicing factor that was shown to interact with exon 7 of SMN, was able to tilt the balance of exon 7 inclusion in the *SMN2* splicing pathway such that the majority of *SMN2* mRNAs were full-length (28).

To gain insights into the mechanism that leads to *SMN2* exon 7 skipping, we have evaluated and compared the relative strength of exon 7 splice sites. Here we provide evidence that the C to T transition within exon 7 of *SMN2* decreases the intrinsic strength of the upstream 3′ splice site (3′ss) by 2-fold. By contrast, the 5′ splice site (5′ss) of exon 7 is not affected by the nucleotide transition. We conclude that the competition between the 3′ss of exons 7 and 8 to pair with the 5′ss of exon 6 amplifies the relatively minor differences in exon 7 splice site strength. These observations suggested that modulation of the 3′ss competition could provide the means to facilitate the inclusion of exon 7, which contains the authentic translation stop codon into the *SMN2*-splicing pathway. We find that the application of antisense oligonucleotides that reduce the recognition of the 3′ splice site of exon 8 increases the incorporation of exon 7 into the fully processed transcript.

MATERIALS AND METHODS

Plasmids—SMN1 and *SMN2* mini-gene constructs containing exon 6, intron 6, exon 7, intron 7, and exon 8 in a *pCI* mammalian expression vector background were a gift from Elliot Androphy. *SMNΔ8* constructs were generated by deleting a *Not*I and *Xcm*I fragment from the *SMN* mini-gene. *SMNΔ6* was generated through the deletion of a *Pst*I and *Nhe*I fragment of the *SMN* mini-gene. *hetSMN* constructs were generated through *Xho*I and *Bcl*I digestion of the *SMN* mini-gene. The deleted region contained exon 6 and most of intron 6. However, in contrast to the *SMNΔ6* constructs, the *hetSMN* constructs retain a pseudointron inherent to the *pCI* backbone. The pseudointron is located upstream of the *SMN* sequences and contains a 5′ splice site derived from exon 1 of β-globin and a 3′ splice site derived from IgM.

Transfections and Reverse Transcription-PCR Analysis—Human cervical carcinoma (C33a) cells were grown in minimal essential media (BioWhittaker) supplemented with 2 mM glutamine and 10% fetal bovine serum. Transfections were performed using the LipofectAMINE 2000 transfection kit (Life Technologies, Inc.). 1 μg of DNA was used to transfect ~3 × 10^5 cells plated 24 h before transfection. At 24 h post-transfection, cells were harvested, and total RNA was isolated using TRIzol reagent (Life Technologies, Inc.). Total RNA was reverse-transcribed with Moloney murine leukemia virus reverse transcriptase for 1 h at 37 °C using poly-dT priming. Radioactive PCR analysis was then performed with different primer sets to identify spliced products. PCR was done for 20 cycles in the presence of 0.2 mM dNTP supplemented with trace amounts of [α-^{32}P]dATP. Each cycle consisted of a 45-s denaturation step at 94 °C, a 45-s annealing step at 56 °C, and a 90-s extension step at 72 °C. For analysis of transfections with *SMNΔ8*, primers used selectively amplified both unspliced and spliced products. Primers used to amplify unspliced products were pCI-for (5′-GCTAACGCAGTCAGTGCTTC-3′) and pCI-rev (5′-GTATCTTATCATGTCTGCTCG-3′). To amplify spliced products, primers used were Tin6-for (5′-TAATACGACTCACTATAGGCCATATAAAGCTATCTATATATAGC-3′) and pCI-rev. For analysis of transfections with *SMNΔ6* and *het-*

SMN, pCI-for and pCI-rev primers were used. As a normalization control, the hypoxanthine phosphoribosyltransferase gene (*HPRT*) was simultaneously amplified by using the primers HPRT-Fw 5′-AAGGAGATGGGAGGCCAT and HPTR-Rev 5′-GTTGAGAGATCATCTCCACCAAT. Reaction products were boiled and fractionated on a 6% polyacrylamide gel. The resulting bands were visualized and quantitated using a PhosphorImager. The splicing efficiency was calculated after normalization to the internal control HPTR by computing the fraction of spliced product counts over the sum of spliced and unspliced counts. Transfection experiments were repeated at least three times.

Antisense Oligonucleotide Application—Stable cell lines expressing either the wild type *SMN1* or *SMN2* mini-gene were generated by G418 selection. Briefly, C33a cells were co-transfected with the plasmid of interest and pSV_{neo}, a neo selection plasmid (a gift from Dr. Marian Waterman), using the LipofectAMINE 2000 reagent (Life Technologies, Inc.). After 12 h, G418 was added to the medium to a final concentration of 2 mg/ml. Selected clones were sub-cultured and amplified. All antisense oligonucleotides containing 2′-*O*-methyl and phosphorothioate backbone modifications were obtained from Dharmacon Research, Inc., Boulder, CO. Antisense oligonucleotides were added to stable cell lines in exponential growth phase using LipofectAMINE 2000. The final concentration of antisense oligonucleotides in the culture medium was 100 nM unless stated otherwise. Cells were harvested, and total RNA was isolated using TRIzol reagent (Life Technologies, Inc.) 24 h after antisense oligonucleotide addition unless stated otherwise. As a loading control, the hypoxanthine phosphoribosyltransferase gene (*HPRT*) was simultaneously amplified by using the primers HPRT-Fw 5′-AAGGAG ATGGGAGGCCAT and HPTR-Rev 5′-GTTGAGAGATCATCTCCA CCAAT. The sequence of the antisense oligonucleotides directed toward the branch point ($oligo_{bp}$) is 5′-CUUCAUAUGUCAGAGUGUACAG-3′, toward the polypyrimidine tract ($oligo_{py}$) is CCUGCAAAUGAGAAAUUAG, and toward the splice site junction ($oligo_{jnct}$) is CUAGUAUUUCCUGCAAAUGAG.

RESULTS

It has been suggested that differential processing of the *SMN1* and *SMN2* pre-mRNAs is caused by the disruption of an ESE located within exon 7 of the transcript (12, 14). The single nucleotide difference within exon 7 of *SMN1* and *SMN2* is located six nucleotides downstream of the 3′ splice site junction. Whereas the C to T transition does not change the coding sequence of the transcript, the recognition of exon 7 by components of the splicing machinery is severely altered. Less than 20% of *SMN2* pre-mRNAs are spliced to include exon 7, whereas more than 90% of *SMN1* pre-mRNAs are processed to include exon 7. Generally, exon skipping is a consequence of the inability of the splicing machinery to recognize and define the exon (29). Exon definition in turn predominantly relies on the strength of 3′ and 5′ splice site signals flanking the exon. Cis-acting RNA elements like ESEs or exonic splicing silencer elements facilitate this process by recruiting general splicing factors to the adjacent exon/intron junctions, thus augmenting the intrinsic strength of 3′ or 5′ splice site (16, 30). Because the C to T transition in *SMN2* is proposed to disrupt a putative ESE element, it is expected that the efficiency at which the splicing machinery recognizes the 5′ or 3′ splice sites will be reduced. To test this hypothesis, we generated a set of SMN mini-genes that was assayed in cell transfection splicing assays.

The C to T Transition in SMN2 Decreases the Utilization of the 3′ Splice Site of Exon 7—To test the effects the C to T transition has on the strength of the 3′ss or 5′ss of exon 7, we designed two sets of identical mini-genes for *SMN1* and *SMN2* (Fig. 2*A*). *SMNΔ8* lacks the majority of intron 7 and all of exon 8 and, thus, tests the activity of the 3′ss of exon 7. *SMNΔ6* lacks exon 6 and the vast majority of intron 6 and, thus, tests the activity of the 5′ss of exon 7. Compared with the wild type substrate, these pre-mRNAs do not contain competing exons. Therefore, splice site activation leads to a single intron removal event. Processed as well as unprocessed RNA were amplified from total RNA preparations by PCR using intron-specific or exon-specific primer sets (see "Materials and Methods"). In the native context of competing splice sites, processing of the *SMN1* and *SMN2* wild type mini-genes lead to the characteristically strong difference in exon 7 inclusion (Fig. 2, *B* and *C*). However, as demonstrated in Fig. 2*B*, the difference of intron 6 removal was observed to be less pronounced for the *SMN1Δ8* and *SMN2Δ8* mini-genes (*lanes 5* and *6*). Before calculating processing efficiencies, band intensities were normalized to the intensity of an internal control, the amplification product of the hypoxanthine phosphoribosyltransferase gene (*HPRT*) (see "Materials and Methods"). Within a data set of four independent transfection experiments, a reproducible difference in splice site strength was determined to be approximately 2-fold (compare splicing efficiencies of 20 ± 3% for *SMN1Δ8* with 9 ± 2% for *SMN2Δ8*) (Fig. 2*B*, Table I). Thus, the C to T transition in *SMN2* decreases the intrinsic strength of the 3′ss strength of exon 7 by 2-fold.

To investigate if the C to T transition in *SMN2* leads to a decrease in the strength of the 5′ss of exon 7, we compared the *SMNΔ6* substrates. As demonstrated in Fig. 2*C*, the steady state levels of intron 7 removal were observed to be surprisingly low (0.5 ± 0.3% for *SMN1Δ6* and 0.8 ± 0.4% for *SMN2Δ6*, Table I). Because we did not detect a statistically significant difference between the efficiencies of *SMN1Δ6* and *SMN2Δ6* splicing, we conclude that the C to T transition in *SMN2* does not affect the 5′ss strength of exon 7 within the context of the single intron pre-mRNA.

The experiments described above indicate that the 3′ss of exons 7 and 8 compete to pair with the 5′ss of exon 6. To evaluate the importance of exon 6 nucleotides in this competition we exchanged exon 6 of SMN with exon 1 derived from β-globin to generate a heterologous substrate, *hetSMN* (Fig. 2*A*). As summarized in Table I, quantitative analysis of the transfection assays shows that the ratio of exon 7 inclusion observed for the *hetSMN* pre-mRNAs are very similar to the levels observed with the wild type SMN mini-genes (Table I). We conclude that the decision to include or exclude exon 7 into the splicing pathway is independent of the nature of the upstream exon and its 5′ splice site. Taken together, these results demonstrate that the nucleotide difference in *SMN2* decreases the utilization of the 3′ss but not of the 5′ss of exon 7. Interestingly, the data also suggest that the relatively minor differences in the strength of the *SMN1* and *SMN2* exon 7 splice sites are drastically amplified in the native cis-competition context.

Antisense Oligonucleotide Application to Modulate the Competition of Exon 7 and Exon 8 Increase the Ratio of Exon 7 Inclusion in SMN2—Because a greater number of *SMN2* gene copies in SMA patients correlates with a milder phenotype of SMA, it has been postulated that the low amount of full-length SMN generated from *SMN2* modulates disease severity (7, 8). Alteration of the *SMN2*-splicing pattern to generate higher fractions of full-length SMN gene product may therefore be a promising therapeutic approach to treat SMA. Our mutational analysis suggested that the splicing machinery recognizes and processes exon 7 efficiently in the absence of a splice site choice. Therefore we reasoned that an antisense oligonucleotide directed toward the 3′ splice site of *SMN2* exon 8 could potentially tilt the balance in favor of exon 7 inclusion. As illustrated in Fig. 3A, this antisense oligonucleotide strategy may also lead to intron 7 retention. However, intron 7 retention does not change the coding region for SMN because the translation stop codon is located within the last nucleotides of exon 7. Stable cell lines expressing the *SMN1* and *SMN2* wild type mini-genes were created by G418 selection. The cells were then incubated in the presence of various antisense oligonucleotides designed to hybridize to components of the 3′ss of exon 8, the proposed branch point sequence ($oligo_{bp}$), the polypyrimidine tract (oli-

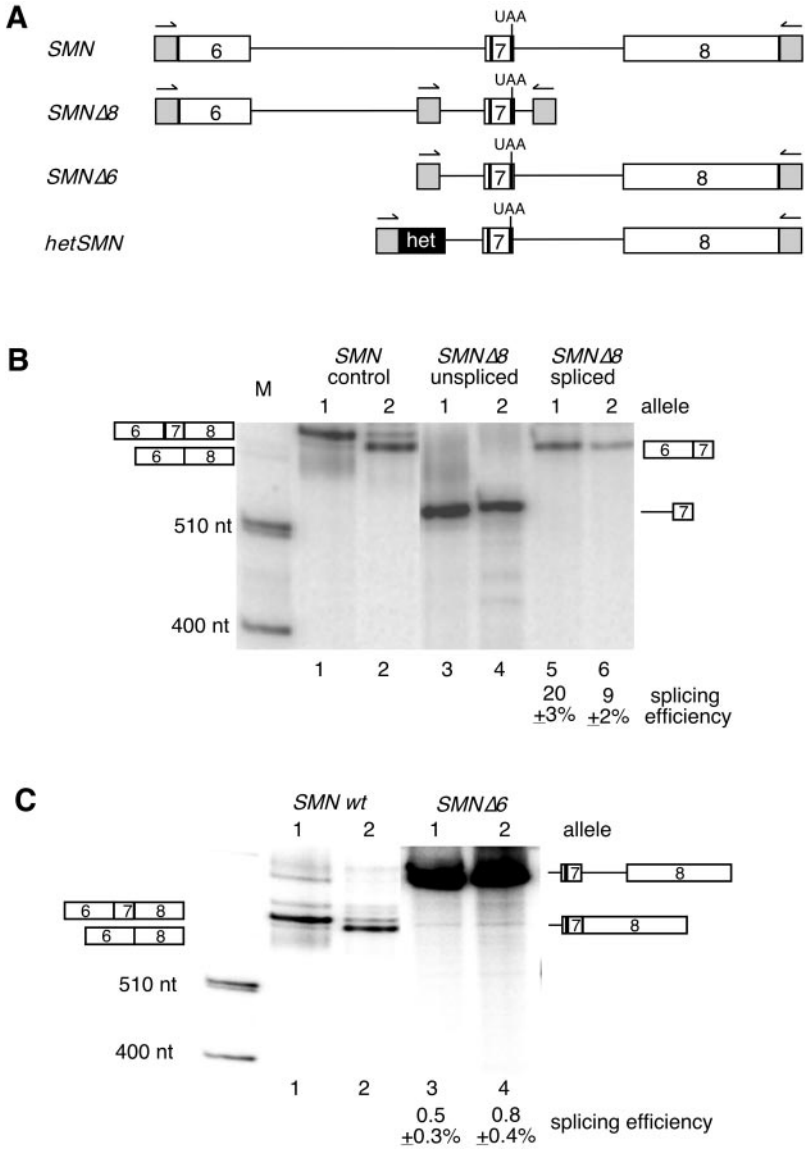

FIG. 2. **Comparison of *SMN1* and *SMN2* exon 7 splice site strength.** *A*, *SMN* substrates tested. *SMNΔ8* and *SMNΔ6* constructs were created by deletion of exon 8 or exon 6, respectively. For *hetSMN* exon 6 was deleted and replaced with a heterologous β-globin sequence containing a functional 5′ splice site. The *gray boxes* show the relative positions of the primer annealing sites. The *arrows* above the *boxes* indicate the directionality of the primer. The *thick bars* within exon 7 highlight the position of the C to T transition and the UAA translation stop codon. *B*, representative autoradiogram of three independent transfection experiments. [α-^{32}P]dATP-labeled reverse transcription-PCR of total RNA isolated from C33a cells 24 h post-transfection with 1 μg of *SMN* or *SMNΔ8* is shown. Different primer sets were used to selectively amplify spliced or unspliced products. *Lanes 1* and *2* are *SMN1* and *SMN2* wild type, and *lanes 3–6* are *SMN1Δ8* and *SMN2Δ8*. Splicing efficiencies for *SMN1Δ8* and *SMN2Δ8* are indicated below *lanes 5* and *6* and represent average values from three independent experiments (20 ± 3% for *SMN1Δ8* with 9 ± 2% for *SMN2Δ8*). *nt*, nucleotides. *M*, molecular mass standards. *C*, reverse transcription-PCR of total RNA isolated from transfection experiments with 1 μg of *SMN* or *SMNΔ6*. *Lanes 1* and *2* are *SMN1*and *SMN2* wild type, and *lanes 3* and *4* are *SMN1Δ6* and *SMN2Δ6*. Splicing efficiencies for *SMN1Δ6* and *SMN2Δ6* are indicated below *lanes 3* and *4* and represent average values from three independent experiments (0.5 ± 0.3% for *SMN1Δ6* and 0.8 ± 0.4% for *SMN2Δ6*).

TABLE I
Splicing efficiency of SMN mini-genes

NA, not applicable.

Substrates	% Splicing efficiency		% Exon 7 inclusion	
	SMN1 allele	SMN2 allele	SMN1 allele	SMN2 allele
SMN	22 ± 3	22 ± 2	92 ± 3	16 ± 2
SMNΔ8	20 ± 3	9 ± 2	NA	NA
SMNΔ6	0.5 ± 0.3	0.8 ± 0.4	NA	NA
hetSMN	12 ± 1	10 ± 2	86 ± 4	14 ± 2

go$_{py}$), or the splice site junction (oligo$_{jnct}$). As illustrated in Fig. 3*B*, treatment of the cell lines with oligo$_{jnct}$, but not with oligo$_{bp}$ (or oligo$_{py}$, data not shown), led to a reproducible increase in the generation of exon 7 containing mRNA. As expected, we also detected a significant fraction of stable SMN RNA that retained intron 7. Quantitative analysis indicates that the antisense oligonucleotide application leads to a 5-fold increase in the ratio of exon 7 inclusion over exon 7 skipping. The absolute levels of exon 7 inclusion increased from 20% in the absence of antisense oligonucleotides up to 50% in the presence of the junction antisense oligonucleotide. Thus, treatment of the stable cell lines expressing the *SMN2* mini-gene with the junction antisense oligonucleotide modulates splice site pairing to include exon 7. As illustrated in Fig. 4*A*, the application of the antisense oligonucleotide is concentration-dependent, with an apparent K_d of 20 ± 10 nM. Maximal splice site modulation is reached at ~100 nM oligo$_{jnct}$. In comparison, incubation of the bp or py antisense oligonucleotides at concentrations of up to 500 nM did not lead to any measurable increase in the fraction of exon 7 inclusion (data not shown). Fig. 4*B* shows a time course of the antisense oligonucleotide treatment. Modulation of *SMN2* splicing is observed within the first 7 h of oligo$_{jnct}$ transfection and is maintained throughout the length of the experiment (72 h). Maximal efficiency was observed after 24 h of treatment, and the steady decrease in antisense activity thereafter is most likely because of the degradation of the 2′ *O*-methyl phosphorothioate oligonucleotide. Although oligo$_{jnct}$ manipulated the ratio of exon 7 inclusion in *SMN2* pre-mRNA

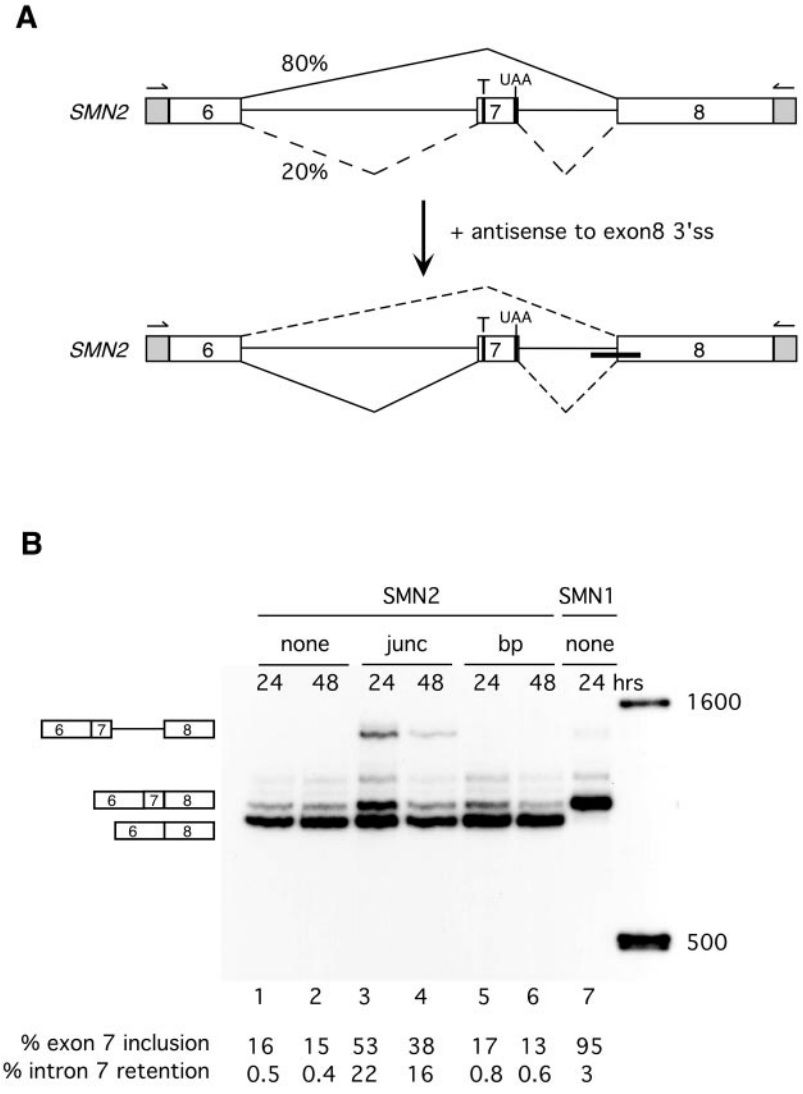

FIG. 3. **Antisense oligonucleotides modulate *SMN2* splicing.** *A*, strategy used to modulate *SMN2* alternative splicing. An antisense oligonucleotide directed toward the intron 7/exon 8 junction reduces the recognition of the exon 8 3′ splice site. As a consequence, the splice site pairing competition between exons 7 and 8 may be tilted to favor exon 7 inclusion. The *thick bars* within exon 7 highlight the position of the C to T transition and the UAA translation stop codon. The *gray boxes* indicate the positions of the primer annealing sites. *B*, the addition of $oligo_{jnct}$ (*lanes 3* and *4*) but not $oligo_{bp}$ (*lanes 5* and *6*) modulates the efficiency of *SMN2* exon 7 inclusion. The percent exon 7 inclusion and intron 7 retention are shown below each lane. Exon 7 inclusion is defined as the sum of fully spliced and intron 7 retained mRNAs. *bp*, base pairs.

splicing, its effect on *SMN1* processing was manifested predominantly by the generation of intron 7 retaining *SMN1* RNAs (data not shown). We conclude that an antisense oligonucleotide treatment directed toward the intron 7/exon 8 junction efficiently and specifically modulates the splicing pattern of *SMN2*.

DISCUSSION

SMA is caused by gross mutations in the telomeric copy of the duplicated SMN genes. The centromeric copy of SMN, *SMN2*, cannot compensate for the loss of *SMN1* because the majority of *SMN2* pre-mRNAs undergo differential RNA splicing. A single C to T nucleotide difference that lies within exon 7 of the SMN transcript leads to preferential exon 7 exclusion in *SMN2*, ultimately leading to production of a truncated and unstable peptide. Thus, the C to T transition drastically affects the efficiency and kinetics at which the splicing machinery recognizes and defines exon 7. To gain insights into the mechanisms by which the C to T transition alters exon 7 definition, we have compared the strength of the *SMN1* and *SMN2* exon 7 splice sites. Our data demonstrate that in the absence of competing splice sites, *i.e.* in the context of a single intron removal event, a 2-fold difference was observed between the 3′ splice sites of *SMN1* and *SMN2*. In contrast, we did not detect a difference between the 5′ splice sites. Thus, the C to T transition does not appear to drastically decrease the intrinsic strength of the exon 7 splice sites. The 2-fold variance clearly cannot account for the greater difference observed in the native context of competing exons. Although 90% of *SMN1* mRNAs include exon 7, only 20% of exon 7-containing mRNAs are observed for *SMN2*. Assuming similar transcriptional activities, the difference in the mole number of full-length SMN mRNAs produced from each SMN locus is therefore approximately 5-fold. To evaluate these differences, it is useful to express the percentage of exon 7 inclusion by the fraction of the apparent rate constant of exon 7 inclusion (k_{inc}) over the apparent rate constant of exon exclusion (k_{ex}). Thus, the fraction of exon 7 inclusion equals k_{inc}/k_{ex}. Because the ratio of exon 7 inclusion is 90% for *SMN1* pre-mRNA processing, the rate of exon inclusion is 9 times faster than the rate of exon skipping. In case of *SMN2*, k_{ex} is 5 times faster than k_{inc}, leading to a 20% inclusion efficiency. In the context of competing exons, k_{inc}/k_{ex} therefore changes from 9 in *SMN1* to 0.2 in *SMN2*, a 45-fold difference. Removal of either intron 6 or intron 7 most likely commits the splicing pattern to exon 7 inclusion. Thus, changes in the rate of exon inclusion depend on the efficiency of either intron 6 or intron 7 splicing. Because our comparison of intron 6 and intron 7 removal indicates that neither process is altered by more than 2-fold, it is tempting to argue that the *SMN2* characteristic exon 7 skipping phenomena arises mainly by increasing the efficiency of the competing exon exclusion reaction. Based on the above comparisons, a 2-fold decrease in the efficiency of intron 6 or intron 7 removal is expected to be

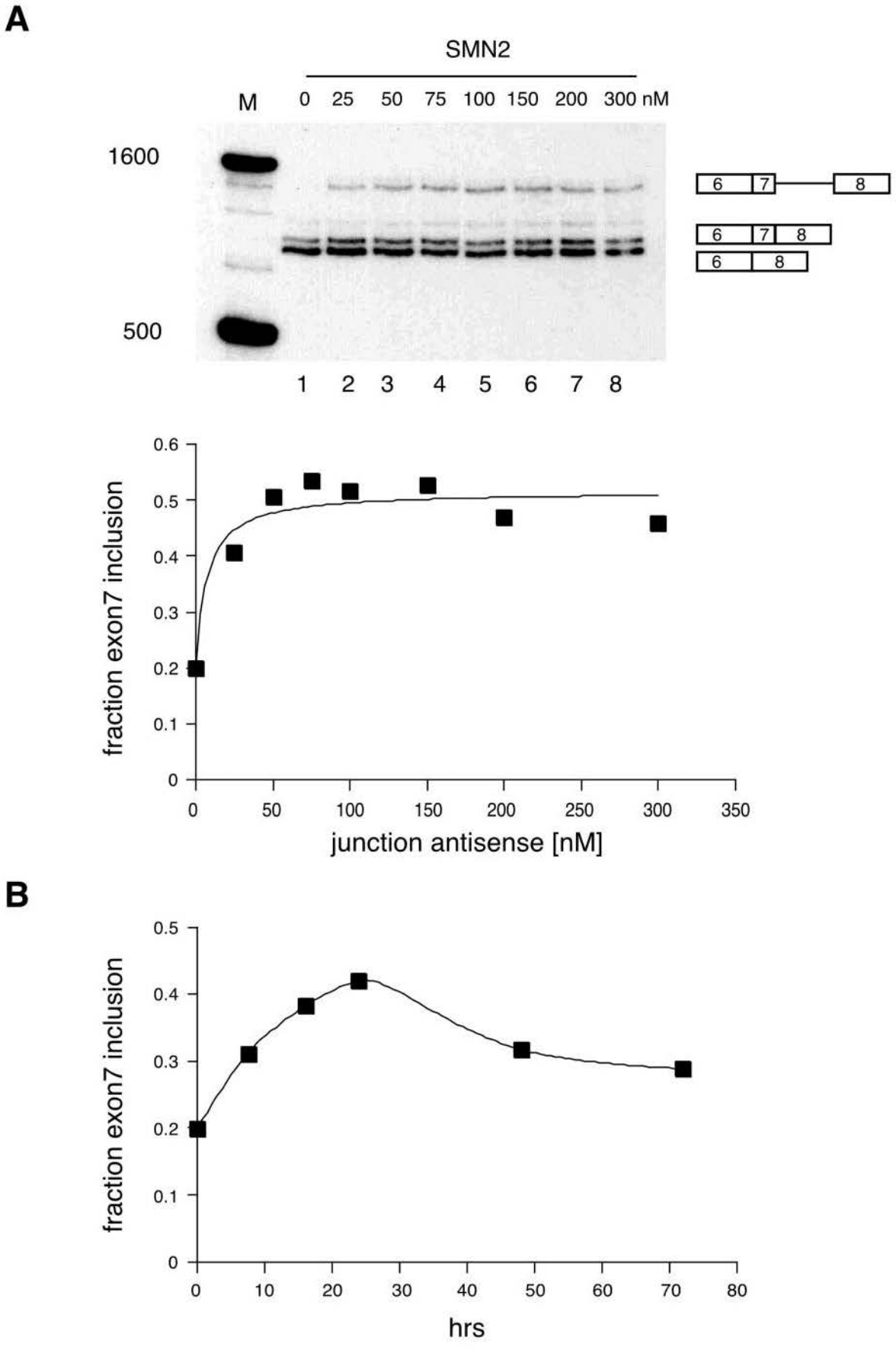

FIG. 4. **Time and concentration dependence of oligo$_{jnct}$ antisense application.** *A*, autoradiogram showing the effects increasing concentrations of oligo$_{jnct}$ has on the splicing pattern of the *SMN2* mini-gene. The quantitation for each concentration tested is shown below. *M*, molecular mass standards. *B*, graph representing the time course of the antisense oligonucleotide application. Oligo$_{jnct}$ was added at a final concentration of 100 nM to *SMN2*-expressing stable cell lines.

accompanied by a 20-fold increase in the rate of k_{ex}. These considerations suggest that a more efficient recognition of exonic sequences by the action of exonic splicing enhancers, for example, affect not only the rate of intron removal but also the competing rate of exon skipping. Therefore, exon definition may incorporate a mechanism that also influences rates of splice site juxtapositioning.

Alternative splicing of the CD45 pre-mRNA has recently been attributed to the combined actions of exonic enhancer and silencer elements (31). It was shown that a single nucleotide polymorphism like SMN, located within exonic sequences, changed the ratio of k_{inc}/k_{ex} by ~30-fold. Using single intron substrates it was further demonstrated that the efficiency of only one of the two intron removal events was altered by approximately 4-fold. By analogy to the above considerations, these results are in agreement with the notion that an increase in the level of exon definition divergently alters the rates of exon inclusion and exon exclusion. A more efficient recognition and assembly of the exonic region by the splicing machinery leads to a less efficient splice site pairing of the upstream splice site with the competing downstream splice site. As demonstrated recently, recruitment of spliceosomal factors to non-splicing competent regions caused inhibition of intron removal.[2] In this case, it was argued that the non-productive splicing complex efficiently competes for splice site pairing across the intron, thereby reducing the probability of a productive juxtapositioning event with a downstream splice site. We would like to suggest that the C to T transition in *SMN2* leads to an overall decrease in the ability of exon 7 to be recognized as exonic. As the affinity of splicing factors to interact with exon 7 decreases, so does the activity of flanking intron removal. In addition, a less defined exon 7 region reduces its ability to prevent exon 7 skipping, and consequently, the competing splice site pairing event between the 5′ splice site of exon 6 and the 3′ splice site of exon 8 becomes the preferred splicing pathway. However, we cannot exclude the possibility that the design of our single intron substrates deleted cis-acting elements required for the full manifestation of the splicing effect caused by the C to T transition.

Our experiments indicate that the C to T transition in *SMN2* does not drastically alter the kinetics of intron 6 or intron 7 removal. If unprocessed and processed SMNΔ8 and SMNΔ6 transcripts are assumed to have similar half-lives, a comparison of their steady state levels strongly suggests that intron 6 removal occurs much faster than intron 7 removal. These conclusions imply that intron 6 removal precedes processing of the terminal intron. Consistent with this interpretation, we reproducibly detect low steady state levels of the *SMN1* intron 7 retaining splicing intermediate (Fig. 3*B*).

Because all individuals with SMA have retained their *SMN2* allele, therapy directed toward increasing *SMN2* exon 7 inclusion could provide a very promising tool to lower the clinical severity of SMA. Our comparison of *SMN1*Δ8 and *SMN2*Δ8 processing demonstrated a low but measurable difference in the efficiency of intron 6 removal. These data suggested that the 3′ss of exon 7 of *SMN1* and *SMN2* have similar affinities for components of the splicing machinery and that the C to T transition in *SMN2* does not abolish the recognition of the 3′ss of *SMN2* exon 7. These observations prompted us to test an antisense oligonucleotide-based approach to modulate the frequency of exon 7 inclusion in *SMN2*. By blocking the 3′ splice site of exon 8 with an antisense probe, we hoped to manipulate the apparent competition between the 3′ splice sites of exon 7 and exon 8. In designing the antisense oligonucleotide, we took advantage of our observation that the 3′ splice site of *SMN2* exon 7 is quite competent to pair with the 5′ splice site of *SMN2* exon 6 and the fact that the SMN translation termination codon resides within exon 7. Of the three tested oligonucleotides, only one, $oligo_{jnct}$, showed any significant effect in modulating *SMN2* exon 7 inclusion. As expected from the experimental design, $oligo_{jnct}$ caused an accumulation of RNA species that retained intron 7. In addition, $oligo_{jnct}$ marginally increased the fraction of fully spliced product. The failure of $oligo_{py}$ and $oligo_{bp}$ to induce any splicing alterations may either be caused by accessibility complications or by their inability to reduce spliceosomal assembly, even when associated with their target sequence. The concentration dependence of $oligo_{jnct}$ illustrates the efficiency of an interaction between $oligo_{jnct}$ and the target sequence. The concentration of $oligo_{jnct}$ required for half-maximal modulation (20 ± 10 nM) favorably compares with other reports utilizing antisense oligonucleotide approaches to alter pre-mRNA-splicing patterns (32–35). As expected from half-life considerations, the $oligo_{jnct}$ splicing effect diminishes over time.

It is unclear at the present time what minimal levels of SMN expression are required to protect against SMA or to prevent the progression of the neuro-degenerate disease. The overall efficiency of the $oligo_{jnct}$ application is illustrated in Fig. 3*B*. At the conditions tested, the presence of the $oligo_{jnct}$ leads to a 2.5-fold increase in the concentrations of RNAs containing exon 7. This numerical increase appears modest in magnitude. However, because it has been demonstrated that increased levels of *SMN2* copy numbers correlate with decreasing severity of SMA, a 2.5-fold increase in the levels of exon 7 containing RNA may be very significant in raising SMN levels to concentrations that allow some level of protection against disease progression. Although the application of $oligo_{jnct}$ demonstrates the feasibility of the antisense approach, it also serves as a stepping stone for the search of related oligonucleotides with higher efficacy.

A recent study demonstrated that the overexpression of hTra2, a human splicing factor that has been shown to interact with an exon 7 ESE common to both *SMN1* and *SMN2* pre-mRNAs, is able to efficiently alter the fraction of exon 7 inclusion in *SMN2* (28). The strategy used in this approach was to increase the probability of an interaction between hTra2 and the pre-mRNA. Activating exon 7 definition in *SMN2* therefore committed the splicing machinery to include exon 7 more frequently into the splicing pattern. Although the results of the exon 7 activation studies were very encouraging, the overexpression of a splicing factor with general functions in pre-mRNA splicing could lead to undesired alterations of other important pre-mRNAs. Here we have tested a splicing modulation approach that by design incorporates a high degree of specificity. The mechanism of $oligo_{jnct}$ action relies on its specific interactions with the 3′ splice site of exon 8. Association of $oligo_{jnct}$ with its target renders it inaccessible for recognition by the splicing machinery. $Oligo_{jnct}$ therefore competes with the splicing machinery for interactions with the 3′ss of exon 8. Although antisense oligonucleotide applications are highly specific in nature, their efficacy depends largely on target accessibility, as demonstrated by the failure of $oligo_{bp}$ and $oligo_{py}$ to affect *SMN2* pre-mRNA splicing. These oligonucleotides in essence served as controls to demonstrate that the processing modulation caused by $oligo_{jnct}$ is a consequence of a specific and productive interaction with the target RNA and not by a non-specific antisense oligonucleotide effect.

Although the antisense approach appears very promising in principle, the ultimate test of the application will be to evaluate if the presence of $oligo_{jnct}$ or a related oligonucleotide leads to

[2] T. D. Schaal, K. J. Hertel , R. Reed, and T. Maniatis, manuscript in preparation.

an increase in the levels of full-length SMN protein. Although $oligo_{jnct}$ directed intron 7 retention will generate a mRNA that, when translated, will produce functional SMN protein, it is unknown if SMN intron 7 retention alters the stability of the RNA or its ability to cross the nuclear membrane. Further experiments will address the outcome of these important issues.

Acknowledgments—We are grateful to Christian Lorson and Elliot Androphy for their generous gift of the *SMN1* and *SMN2* mini-gene plasmids and Marian Waterman for the pSV_{neo} selection plasmid. We thank Jared Salbato for help in designing the antisense oligonucleotides in this study and Ming Tan, Brent Graveley, Marian Waterman, and the Hertel lab for helpful comments on the manuscript.

REFERENCES

1. Roberts, D. F., Chavez, J., and Court, S. D. (1970) *Arch. Dis. Child* **45,** 33–38
2. Pearn, J. H. (1973) *J. Med. Genet.* **10,** 260–265
3. Pearn, J. (1978) *J. Med. Genet.* **15,** 409–413
4. Lefebvre, S., Burglen, L., Reboullet, S., Clermont, O., Burlet, P., Viollet, L., Benichou, B., Cruaud, C., Millasseau, P., Zeviani, M., Le Paslier, D., Frézal, J., Cohen, D., Weissenbach, J., Munnich, A., and Melki, J. (1995) *Cell* **80,** 155–165
5. Rodrigues, N. R., Owen, N., Talbot, K., Ignatius, J., Dubowitz, V., and Davies, K. E. (1995) *Hum. Mol. Genet.* **4,** 631–634
6. Cobben, J. M., van der Steege, G., Grootscholten, P., de Visser, M., Scheffer, H., and Buys, C. H. (1995) *Am. J. Hum. Genet.* **57,** 805–808
7. Coovert, D. D., Le, T. T., McAndrew, P. E., Strasswimmer, J., Crawford, T. O., Mendell, J. R., Coulson, S. E., Androphy, E. J., Prior, T. W., and Burghes, A. H. (1997) *Hum. Mol. Genet.* **6,** 1205–1214
8. Lefebvre, S., Burlet, P., Liu, Q., Bertrandy, S., Clermont, O., Munnich, A., Dreyfuss, G., and Melki, J. (1997) *Nat. Genet.* **16,** 265–269
9. Burghes, A. H. (1997) *Am. J. Hum. Genet.* **61,** 9–15
10. Melki, J. (1997) *Curr. Opin. Neurol.* **10,** 381–385
11. McAndrew, P. E., Parsons, D. W., Simard, L. R., Rochette, C., Ray, P. N., Mendell, J. R., Prior, T. W., and Burghes, A. H. (1997) *Am. J. Hum. Genet.* **60,** 1411–1422
12. Monani, U. R., Lorson, C. L., Parsons, D. W., Prior, T. W., Androphy, E. J., Burghes, A. H., and McPherson, J. D. (1999) *Hum. Mol. Genet.* **8,** 1177–1183
13. Lorson, C. L., Strasswimmer, J., Yao, J. M., Baleja, J. D., Hahnen, E., Wirth, B., Le, T., Burghes, A. H., and Androphy, E. J. (1998) *Nat. Genet.* **19,** 63–66
14. Lorson, C. L., Hahnen, E., Androphy, E. J., and Wirth, B. (1999) *Proc. Natl. Acad. Sci. U. S. A.* **96,** 6307–6311
15. Fu, X.-D. (1995) *RNA* (*N. Y.*) **1,** 663–680
16. Hertel, K. J., Lynch, K. W., and Maniatis, T. (1997) *Curr. Opin. Cell Biol.* **9,** 350–357
17. Graveley, B. R. (2000) *RNA* (*N. Y.*) **6,** 1197–1211
18. Rio, D. C. (1992) *Gene Expr.* **2,** 1–5
19. Ruskin, B., Zamore, P. D., and Green, M. R. (1988) *Cell* **52,** 207–219
20. Zamore, P. D., and Green, M. R. (1989) *Proc. Natl. Acad. Sci. U. S. A.* **86,** 9243–9247
21. Zorio, D. A., and Blumenthal, T. (1999) *Nature* **402,** 835–838
22. Wu, S., Romfo, C. M., Nilsen, T. W., and Green, M. R. (1999) *Nature* **402,** 832–835
23. Merendino, L., Guth, S., Bilbao, D., Martinez, C., and Valcarcel, J. (1999) *Nature* **402,** 838–841
24. Wang, Z., Hoffmann, H. M., and Grabowski, P. J. (1995) *RNA* **1,** 21–35
25. Zuo, P., and Maniatis, T. (1996) *Genes Dev.* **10,** 1356–1368
26. Graveley, B. R., Hertel, K. J., and Maniatis, T. (2001) *RNA* (*N. Y.*) **7,** 806–818
27. Lorson, C. L., and Androphy, E. J. (2000) *Hum. Mol. Genet.* **9,** 259–265
28. Hofmann, Y., Lorson, C. L., Stamm, S., Androphy, E. J., and Wirth, B. (2000) *Proc. Natl. Acad. Sci. U. S. A.* **97,** 9618–9623
29. Berget, S. M. (1995) *J. Biol. Chem.* **270,** 2411–2414
30. Blencowe, B. J. (2000) *Trends Biochem. Sci.* **25,** 106–110
31. Lynch, K. W., and Weiss, A. (2001) *J. Biol. Chem.* **276,** 24341–24347
32. Dunckley, M. G., Manoharan, M., Villiet, P., Eperon, I. C., and Dickson, G. (1998) *Hum. Mol. Genet.* **7,** 1083–1090
33. Friedman, K. J., Kole, J., Cohn, J. A., Knowles, M. R., Silverman, L. M., and Kole, R. (1999) *J. Biol. Chem.* **274,** 36193–36199
34. Taylor, J. K., Zhang, Q. Q., Wyatt, J. R., and Dean, N. M. (1999) *Nat. Biotechnol.* **17,** 1097–1100
35. Mercatante, D. R., Bortner, C. D., Cidlowski, J. A., and Kole, R. (2001) *J. Biol. Chem.* **276,** 16411–16417

GENES: STRUCTURE AND REGULATION:

Modulation of Survival Motor Neuron Pre-mRNA Splicing by Inhibition of Alternative 3′ Splice Site Pairing

Sharlene R. Lim and Klemens J. Hertel

J. Biol. Chem. 2001, 276:45476-45483.
doi: 10.1074/jbc.M107632200 originally published online October 2, 2001